Contribution from the Department of Chemistry,
Texas A&M University, College Station, Texas 77843

Synthesis and Characterization of Binuclear Manganese Complexes: Redox Models for the Water Oxidation Cofactor of Photosystem II

Takayuki Matsushita, Lee Spencer, and Donald T. Sawyer*

Received July 2, 1987

Binuclear manganese complexes have been prepared (a) via the use of bridging quadradentate bis(Schiff bases) and dipicolinates and (b) with bis(μ-oxo) groups and one or two picolinate ligands per manganese. Their redox chemistry, which has been characterized by cyclic voltammetry and controlled-potential coulometry, indicates that the electron-transfer mechanisms are ligand-centered rather than metal-centered. Several of the complexes appear to be effective reaction mimics and models for the manganese cofactor in photosystem II that facilitates water oxidation to dioxygen.

Binuclear manganese centers have been proposed for the water oxidation site of photosystem II as well as for several other redox active proteins.[1-4] This has prompted the synthesis and characterization of various manganese model compounds.[5-7] From this group the redox chemistry for several neutral manganese(III) complexes [$Mn^{III}L_3$, where L = acetylacetonate (acac), 2-picolinate (PA), and 8-quinolinate (8-Q)] has been determined in acetonitrile.[8] Numerous Schiff-base complexes of manganese also have been used as spectroscopic probes for the active site of PSII.[9-13]

The majority of model manganese complexes have been mononuclear and undergo single-electron-transfer redox processes. However, the redox potential for the initial one-electron oxidation of water ($H_2O \rightarrow {}^{\bullet}OH + H^+ + e^-$) is +2.31 V vs NHE (at pH 7).[14] The magnitude of this potential and the high reactivity[15] of the hydroxyl radical ($^{\bullet}OH$) restricts the mechanism of photosynthetic water oxidation to either two concerted two-electron oxidations or a single concerted four-electron oxidation of water.[16] Thus, a polynuclear manganese center appears to be necessary to facilitate the overall four-electron oxidation of water to dioxygen ($2H_2O \rightarrow O_2 + 4H^+ + 4e^-$; $E^{\circ\prime}_{pH7}$, +0.81 V vs NHE).

Two binuclear manganese complexes,[17,18] tetrakis(1,10-phenanthroline)bis(μ-oxo)dimanganese(IV) perchlorate $[Mn^{IV}_2O_2(phen)_4](ClO_4)_4$ and tetrakis(2,2′-bipyridyl)bis(μ-oxo)dimanganese(IV,III) perchlorate $[Mn^{III}Mn^{IV}O_2(bpy)_4](ClO_4)_3$, have been used as models of the active site of PSII in conjunction with EXAFS and other spectroscopic studies.[19,20] However, the redox potentials of these compounds are beyond the limits of the photon-induced charge separation of PSII.[21]

The goal of the present study has been to prepare new binuclear manganese complexes with two-electron-redox chemistry that is compatible with the *reversible* oxidation of water to oxygen. Three approaches have been taken: (i) use of bridging Schiff-base ligands combined with suitable mononuclear manganese precursors to form discrete binuclear compounds via ligand-displacement reactions; (ii) use of a bridging ligand with two picolinate anion groups to bind two mononuclear manganese precursors to form binuclear model compounds; (iii) modification of the ligand environment of $[Mn^{III}Mn^{IV}O_2(bpy)_4](ClO_4)_3$ via substitution by picolinate anion (PA^-) to generate a bis(μ-oxo)-bridged manganese complex with redox potentials tuned to model the redox catalysis of the manganese cofactor of PSII.

The redox chemistry of these binuclear complexes has been characterized by electrochemical and spectroscopic measurements. The results indicate that their electron-transfer mechanisms involve a ligand-centered rather than a metal-centered process.[2,22,23] The applicability of this type of mechanism to that of photosynthetic water oxidation is discussed.

Experimental Section

Equipment. A three-electrode potentiostat (Bioanalytical Systems Model CV-27) was used for the cyclic voltammetry and controlled-potential electrolysis experiments. The cyclic voltammograms were recorded on a Houston Instruments Model 200 XY recorder. The experiments were conducted in a 15-mL electrochemical cell with provision to control the presence of oxygen with an argon purge system. The working electrode was a Bioanalytical Systems glassy-carbon inlay (area, 0.09 cm^2); the auxillary electrode a platinum wire; and the reference electrode a Ag/AgCl wire in an aqueous tetramethylammonium chloride solution that was adjusted to give a potential of 0.00 V vs SCE. The latter was contained in a Pyrex tube with a cracked soft-glass tip, which was placed inside a luggin capillary.[24]

A Hewlett-Packard Model 8450A diode-array spectrophotometer was used for the UV–visible spectrophotometric measurements, and the NMR spectra were recorded with 90- and 200-MHz Varian spectrometers. The IR spectra were recorded with a Perkin-Elmer spectrometer and the gas chromatographic analyses were accomplished with a Hewlett-Packard Model 5880 gas chromatograph.

Reagents. The chemicals and solvents for the investigations and syntheses were the highest purity commercially available and were used without further purification, except as noted: tetraethylammonium perchlorate (TEAP, G. Frederick Smith), tetrabutylammonium hydroxide ((TBA)OH, Aldrich), picolinic acid (PAH, Aldrich), 2,4-pentanedione (acac, Aldrich), 2,2′-bipyridine (bpy, Aldrich), 1,2-bis(4-pyridyl)ethane [$C_2(py)_2$, Aldrich], 4,4′-trimethylenedipyridine [$C_3(py)_2$, Aldrich], sodium cyanide (Aldrich), $Mn^{II}(OAc)_3 \cdot 2H_2O$ (Aldrich), salicylaldehyde (sal, Aldrich), 1,2-ethanediamine (en, Aldrich), 1,3-

(1) Dekker, J. P.; Van Gorkom, H. J.; Wensink, J.; Ouwehand, L. *Biochim. Biophys. Acta* **1984**, *767*, 1.
(2) Renger, G.; Weiss, W. *Biochim. Biophys. Acta* **1986**, *850*, 184.
(3) Kambara, T.; Govindjee. *Proc. Natl. Acad. Sci. U.S.A.* **1985**, *82*, 6119.
(4) Brudvig, G. W.; Crabtree, R. H. *Proc. Natl. Acad. Sci. U.S.A.* **1986**, *83*, 4586.
(5) Lynch, M. W.; Hendrickson, D. N.; Fitzgerald, B. J.; Pierpont, C. G. *J. Am. Chem. Soc.* **1984**, *106*, 2041.
(6) Kirby, J. A.; Robertson, A. S.; Smith, J. P.; Thompson, A. C.; Cooper, S. R.; Klein, M. P. *J. Am. Chem. Soc.* **1981**, *103*, 5529.
(7) Yamaguchi, K. S.; Sawyer, D. T. *Isr. J. Chem.* **1985**, *25*, 164.
(8) Yamaguchi, K. S.; Sawyer, D. T. *Inorg. Chem.* **1985**, *24*, 971.
(9) Matsushita, T.; Shono, T. *Bull. Chem. Soc. Jpn.* **1981**, *54*, 2646.
(10) Matsushita, T.; Shono, T. *Bull. Chem .Soc. Jpn.* **1982**, *55*, 108.
(11) Coleman, W. M. *Inorg. Chim. Acta* **1981**, *49*, 205.
(12) Bouncher, L. J.; Day, V. W. *Inorg. Chem.* **1977**, *16*, 1360.
(13) Kessissoglou, D. P.; Butler, W. M.; Pecoraro, V. L. *J. Chem. Soc., Chem. Commun.* **1986**, 1253.
(14) Hoare, J. P. In *Standard Potentials in Aqueous Solution*; Bard, A. J., Parsons, R., Jordan, J., Eds.; Marcel Dekker: New York, 1985; pp 49–66.
(15) Walling, C. *Acc. Chem. Res.* **1975**, *8*, 125.
(16) Spencer, L.; Sawyer, D. T.; Webber, A. N.; Heath, R. L. In *Progress in Photosynthesis Research*; Biggens, J., Ed.; Martinus Nijhoff: Dordrecht, Holland, 1987; Vol. I, pp 717–720.
(17) Goodwin, H. A.; Sylva, R. N. *Aust. J. Chem.* **1967**, *20*, 629.
(18) Nyholm, R. S.; Turco, A. *Chem. Ind. (London)* **1960**, 74.
(19) Cooper, S. R.; Calvin, M. *J. Am. Chem. Soc.* **1977**, *99*, 6623.
(20) Cooper, S. R.; Dismukes, G. C.; Klein, M. P.; Calvin, M. *J. Am. Chem. Soc.* **1978**, *100*, 7248.
(21) Morrison, M. M.; Sawyer, D. T. *J. Am. Chem. Soc.* **1977**, *99*, 257.
(22) Goodin, D. B.; Yachandra, V. K.; Britt, R. D.; Sauer, K.; Klein, K. *Biochim. Biophys. Acta* **1984**, *767*, 209.
(23) Padhye, S.; Kambara, T.; Hendrickson, D. N.; Govindjee. *Photosynth. Res.* **1986**, *9*, 103.
(24) Sawyer, D. T.; Roberts, J. L., Jr. *Experimental Electrochemistry for Chemists*; Wiley-Interscience: New York, 1974; p 144.

0020-1669/88/1327-1167$01.50/0

propanediamine (pn, Aldrich), 1,4-butanediamine (bn, Aldrich), 1,5-hexanediamine (hxn, Aldrich), *m*-xylenediamine (*m*-Xyln, Aldrich), and *n*-octylamine (Octn, Aldrich). The solvents for all of the experiments were "distilled in glass" grade dimethyl sulfoxide (Me_2SO), dimethylformamide (DMF), acetonitrile (MeCN), and pyridine (py) from Burdick and Jackson. High-purity argon gas was used to deaerate the solutions.

Preparation of Complexes. Several manganese(III) complexes were prepared by conventional methods: $[Mn^{III}(acac)_3]$,[25] $[Mn^{III}(PA)_3]$,[8] $[Mn^{III}(PA)_2(acac)]$,[8] and $[(bpy)_2Mn^{III}(\mu\text{-}O)_2Mn^{IV}(bpy)_2](ClO_4)_3$.[18] The magnetic susceptibility of the latter two compounds was measured by the Gouy method at 19.8 °C (corrected): $[Mn^{III}(PA)_2(acac)]$, 4.88 μ_B/molecule; $[(bpy)_2Mn^{III}(\mu\text{-}O)_2Mn^{IV}(bpy)_2](ClO_4)_3$, 2.52 μ_B/molecule.

(*N*,*N*′-Disalicylidenepropanediaminato)manganese(III) Chloride, [Mn^{III}(salpn)(Cl)]. To a solution of *N*,*N*′-disalicylidenepropanediamine (salpnH_2, 2.82 g, 10 mmol) in methanol (100 mL) was added $Mn^{III}(OAc)_3\cdot 2H_2O$ (2.68 g, 0.01 mol) and LiCl (0.63 g, 15 mmol). The mixture was refluxed for 1 h and then evaporated to dryness. The residue was washed with 2-propanol and then ether and dried in vacuo. The resulting product was recrystallized from acetonitrile. Anal. Calcd for $MnC_{14}H_{16}N_2O_2Cl\cdot 0.5H_2O$: C, 53.74; H, 4.51; N, 7.37; O, 10.53; Cl, 9.33. Found: C, 53.72; H, 5.01; N, 6.99; O, 10.77, Cl, 9.05.

Tetramethylammonium Bis(μ-oxo)tetrakis(2-picolinato)dimanganate(III,IV), $(Me_4N)(\mu,\mu'\text{-}O_2[Mn^{IV/III}(PA)_2]_2)$. To a solution of $[(bpy)_2Mn^{III}(\mu\text{-}O)_2Mn^{IV}(bpy)_2](ClO_4)_3$ (0.551 g, 0.5 mmol) in MeCN (70 mL) was added a solution of tetramethylammonium picolinate [(Me$_4$N)PA, 0.412 g (2.1 mmol)] in MeCN (50 mL). The solution was stirred at room temperature for 1 h and concentrated to 30 mL under reduced pressure. The resulting precipitate was removed by filtration and the filtrate concentrated to 10 mL to give a dark green precipitate. This was collected on a glass filter, washed with MeCN, acetone, and ether, and dried in vacuo (yield, 0.22 g). Anal. Calcd for $Mn_2C_{28}H_{28}N_5O_{10}$: C, 46.55; H, 4.18; N, 9.69. Found: C, 46.38; H, 3.89; N, 9.49. Magnetic susceptibility: 3.04 μ_B/ molecule (Gouy method at 19.8 °C).

Bis(μ-oxo)tetrakis(2-picolinato)dimanganese(IV), $[\mu,\mu'\text{-}O_2[Mn^{IV}(PA)_2]_2]$. This complex was prepared by a slight modification of the synthetic procedure for $[Mn^{III/IV}(bpy)_2O]_2(ClO_4)_3\cdot H_2O$.[18] To a solution of $Mn^{II}(OAc)_2\cdot 4H_2O$ (1.84 g, 7.5 mmol) in H_2O (30 mL) were added picolinic acid (3.26 g, 26.5 mmol) and acetate buffer solution (9 mL, pH 4.5). A solution of $KMnO_4$ (0.79 g, 5 mmol) in H_2O (25 mL) was added dropwise with stirring at 0 °C. The mixture was stirred for 1 h at 0 °C and the resulting olive green precipitate was collected on a glass filter, washed with EtOH and then ether, and dried in vacuo (yield, 5.5 g). This complex is slightly soluble in DMF, Me_2SO, and CH_2Cl_2 but insoluble in MeCN. The synthesis of an insoluble material with an equivalent formula has been described.[26]

This complex also was prepared by displacement of $[(\mu'\text{-}O)_2[Mn^{IV}(phen)_2]_2(ClO_4)_4\cdot H_2O$ with (Me$_4$N)(PA): To a red-brown solution of this complex (0.639 g, 0.5 mmol) in MeCN (50 mL) was added dropwise a solution of (Me$_4$N)(PA) (0.412 g, 2.1 mmol) in MeCN (50 mL) at room temperature with stirring. The resulting red-brown solution turned greenish brown, and a brown precipitate deposited after 20 min. This was collected on a glass filter, washed with MeCN and ether, and dried in vacuo (yield, 72 mg). Anal. Calcd for $Mn_2C_{24}H_{16}N_4O_{10}$: C, 45.74; H, 2.56; N, 8.89. Found: C, 45.88; H, 2.75; N, 8.87. Magnetic susceptibility: 2.31 μ_B/molecule (Gouy method at 19.8 °C).

Preparation of Bridging Ligands. The Schiff base ligands salen, salpn, salbn, salhn, and sal-*m*-Xyln (see Figure 1) were prepared by the condensation reaction of salicylaldehyde and the appropriate diamine in ethanol. The products were recrystallized from ethanol or tetrahydrofuran and dried in vacuo before use. The ligand 5,5′-methylenedisalicylaldehyde (disalH_2) was prepared by the method of Marvel and Tarkoy.[27] The Schiff-base derivative 5,5′-methylenebis(*N*-octylsalicylideneamine) (*N*-oct-disalH_2) was obtained by condensation of disalH_2 with *n*-octylamine in THF. The ligand was recrystallized from a mixed solvent of CH_2Cl_2 and EtOH (1:2).

4,4′-Trimethylenebis(pyridine *N*-oxide), $[C_3(pyO)_2]$. 4,4′-Trimethylenedipyridine (40 g) was placed in a 500-mL three-necked round-bottom flask that contained glacial acetic acid (200 mL). The solution was warmed to 70 °C, and aqueous hydrogen peroxide solution (30%, 32 mL) was added dropwise with stirring. The solution was stirred for 7 h at 70 °C, additional HOOH (32 mL) was added, and the solution was stirred for 48 h at 70 °C. The resulting solution was evaporated under reduced pressure to give a pale yellow solid. (The absence of residual hydrogen peroxide in the solution was confirmed prior to evaporation to dryness.) The resulting compound was recrystallized from MeOH; yield 42.8 g.

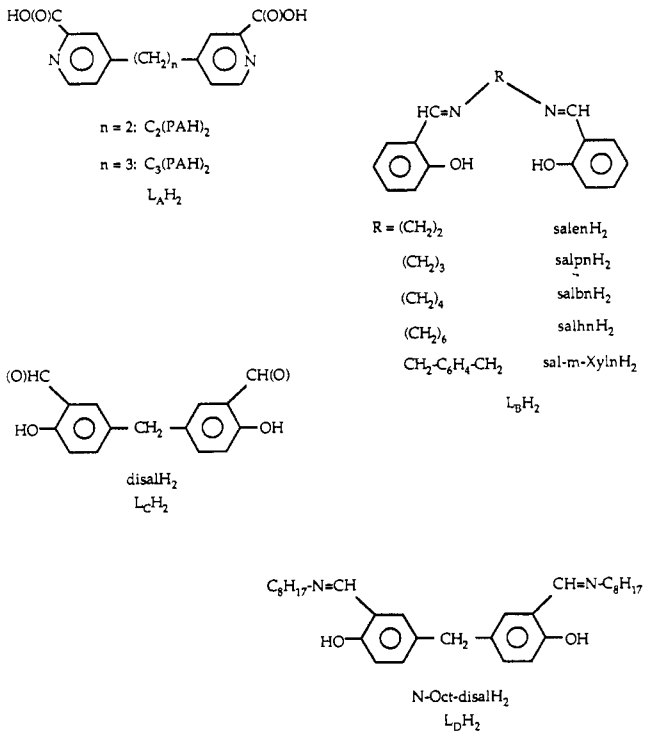

Figure 1. Bridging ligands.

4,4′-Trimethylenebis(2-cyanopyridine), $[C_3(pyCN)_2]$. 4,4′-Trimethylenebis(pyridine *N*-oxide) (9.2 g, 40 mmol) was placed in a 50-mL three-necked round-bottom flask equipped with a thermometer and a condenser. Dimethyl sulfate [$(MeO)_2SO_2$, 5.06 mL] was added dropwise with stirring, and then the mixture was warmed gradually to about 50 °C to give a molten salt. Next, an additional 2.54 mL of $(MeO)_2SO_2$ was added dropwise and the mixture warmed to 90 °C for 2 h with stirring. [Because this reaction is highly exothermic, the addition of $(MeO)_2SO_2$ must be done with care. Avoid rapid addition and do not heat the mixture above 90 °C.] After being cooled to room temperature, the solution was evaporated for 2 h with an aspirator to give a pale brown solid ($[CH_3ONC_5H_4(CH_2)_3C_5H_4NOCH_3][(CH_3O)SO_2]_2$).

Next, nitrile groups were introduced at the 2-position of the pyridine rings of this salt.[28] Sodium cyanide (16 g) was dissolved in H_2O (32 mL) in a 300-mL three-necked round-bottom flask equipped with a thermometer and an inlet and outlet for Ar gas. After Ar gas had been passed through the flask for 30 min and the solution was cooled to 0 to −5 °C, the dipyridyl salt in 12 mL of H_2O was added dropwise under an Ar atmosphere to give a green solution, which was stirred for 3 h at −5 °C. The resulting solution was kept in a refrigerator overnight, during which a brown precipitate formed. This mixture was extracted four times with CH_2Cl_2 (150 mL); the extracts were dried over $MgSO_4$ and distilled under vacuum to give a yellowish orange oil. The latter was purified by column chromatography in CH_2Cl_2–acetone (50:50) on a column of silica gel (100–200 mesh, 2.0 × 50 cm). An orange solid was obtained after removal of the eluent, which was recrystallized from a mixture of acetone and petroleum ether; yield 1.8 g.

4,4′-Trimethylenebis(2-pyridinecarboxylic acid), $[C_3(PAH)_2]$. 4,4′-Trimethylenebis(2-cyanopyridine) (1.0 g) was dissolved in 6 M HCl (50 mL), refluxed for 6 h with stirring, and then stirred overnight at room temperature. The resulting solution was evaporated to dryness under reduced pressure to give a brown solid, 4,4′-trimethylenebis(2-carboxypyridinium chloride). This was dissolved in H_2O (20 mL) and the solution adjusted to pH 4.0 with 1 M NaOH before it was evaporated to dryness under reduced pressure. The resulting brown solid was extracted with absolute MeOH (100 mL) and treated with activated charcoal, and the MeOH solution again was evaporated to dryness and extracted with DMF (50 mL). The DMF solution was concentrated to 15 mL, and the precipitated NaCl was removed by filtration. The filtrate was reprecipitated with a mixture of 2-propanol and diethyl ether (30/70, 50 mL). This procedure was repeated twice to remove residual NaCl; yield 0.6 g.

(25) Berg, W.; Truemper, T. J. *J. Phys. Chem.* **1960**, *64*, 487.
(26) Hoof, D. L.; Tisley, D. G.; Walton, R. A. *Inorg. Nucl. Chem. Lett.* **1973**, *9*, 571.
(27) Marvel, C. S.; Tarkoy, N. *J. Am. Chem. Soc.* **1957**, *79*, 6000.
(28) Feely, W. E.; Beavers, E. M. *J. Am. Chem. Soc.* **1959**, *81*, 4004.

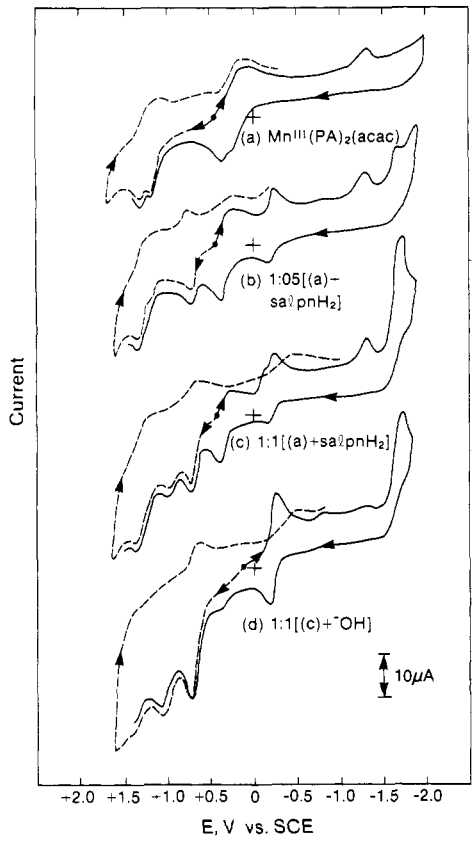

Figure 2. Electrochemical titration of 1 mM $Mn^{III}(PA)_2(acac)$ with $salpnH_2$ in MeCN (0.1 M TEAP) at a glassy-carbon electrode.

Results

The bridging ligands include dipicolinic acid derivatives (L_AH_2), a series of tetradentate Schiff-base ligands (L_BH_2), and the Schiff-base condensation product (L_pH_2) of disalicylaldehyde (L_2H_2) and *n*-octylamine (see Figure 1). The approach to the preparation of discrete binuclear Mn(III) complexes has been the combination of a bridging ligand with the mononuclear Mn(III) precursors $[Mn^{III}(PA)_2(acac)]$ and $[Mn^{III}(salpn)Cl]$ whereby the acac and chloro ligands are displaced.

Reaction of $[Mn^{III}(PA)_2(acac)]$ with $salpnH_2$ and $salenH_2$. The electrochemistry of $[Mn^{III}(PA)_2(acac)]$ is illustrated by the cyclic voltammograms of Figure 2a; the potentials for the reversible reduction and oxidation reactions are summarized in Table I. Similar electrochemistry is observed for this complex in dimethylformamide solutions.

Upon addition of 0.5 equiv of $salpnH_2$ (in MeCN), the solution color changes from wine red to olive green, the voltammetric waves for $[Mn^{III}(PA)_2(acac)]$ decrease in intensity, and new reversible reduction and oxidation waves appear at −0.22 and +0.73 V vs SCE, respectively, as well as an irreversible oxidation wave at +1.10 V (Figure 2b). The peak currents for these new waves increase upon addition of another 0.5 equiv of $salpnH_2$ (Figure 2c). A similar pattern occurs when $salenH_2$ is added to $[Mn^{III}(PA)_2(acac)]$. The addition of 1.0 equiv of base $(Bu_4N)OH$ to a 1:1 mixture of $salpnH_2$ and $[Mn^{III}(PA)_2(acac)]$ in MeCN causes the formation equilibrium to be driven to the right; the reversible couple for $[Mn^{III}(PA)_2(acac)]$ completely disappears, and the peak currents for the product reach a maximum.

The absorption spectrum for $[Mn^{III}(PA)_2(acac)]$ (Figure 3, solid line) includes a shoulder at 520 nm and a maximum at 323 nm (ϵ = 6620 M^{-1} cm^{-1}).[8] Addition of $salpnH_2$ to this complex results in a new absorption peak at 576 nm. As in the electrochemical study, the maximum concentration of product is obtained after the addition of 1.0 equiv of $salpnH_2$ (or $salenH_2$) and no significant increase was observed on addition of additional $salpnH_2$.

Reaction of $[Mn^{III}(PA)_2(acac)]$ with *N*-Oct-$disalH_2$, $salhnH_2$, sal-*m*-$XylnH_2$, and $disalH_2$. Figure 4 illustrates the cyclic voltammograms that result from the addition of 0.5 and 1.0 equiv of the ligand *N*-Oct-$disalH_2$ to $[Mn^{III}(PA)_2(acac)]$. An initial negative scan yields two irreversible reductions at 0.00 and −0.28 V vs SCE, and an initial positive scan yields two irreversible oxidations at +1.05 and +1.40 V vs SCE. Addition of $^-$OH causes the first reduction wave to disappear. Similar results are observed for the other bridging ligands in this study; the redox potentials are summarized in Table I.

The changes in the UV/visible spectra that result from the addition of *N*-oct-$disalH_2$ to $[Mn^{III}(PA)_2(acac)]$ provide persuasive evidence for formation of a new complex with two metals bridged by the ligand (Figure 5; isosbestic points at 540 nm and 565 nm, and a maximum for the product at 664 nm (ϵ = 180 M^{-1} cm^{-1})). The reaction stoichiometry is 1.0 equiv of ligand per 2.0 Mn as demonstrated by the small changes in the absorbance when additional ligand is added. Similar stoichiometries are observed for the other bridging ligands; the spectroscopic data are summarized in Table I.

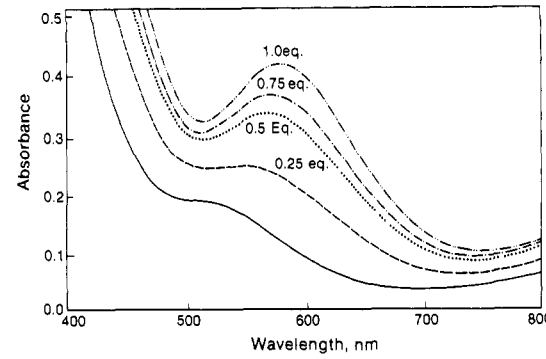

Figure 3. Spectrophotometric titration of 1 mM $Mn^{III}(PA)_2(acac)$ with $salpnH_2$ in MeCN. Further addition of $salpnH_2$ does not affect the spectrum.

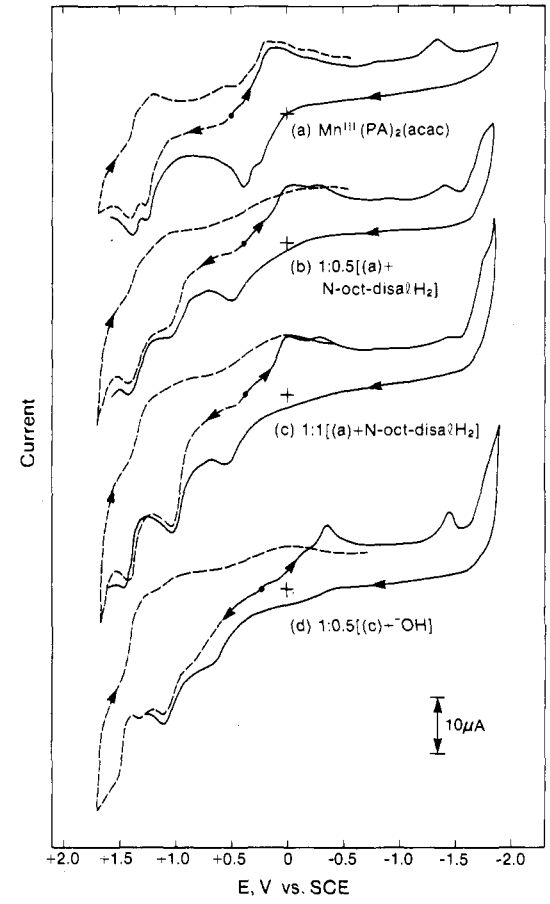

Figure 4. Electrochemical titration of 1 mM $Mn^{III}(PA)_2(acac)$ with *N*-Oct-$disalH_2$ in MeCN (0.1M TEAP) at a glassy-carbon electrode.

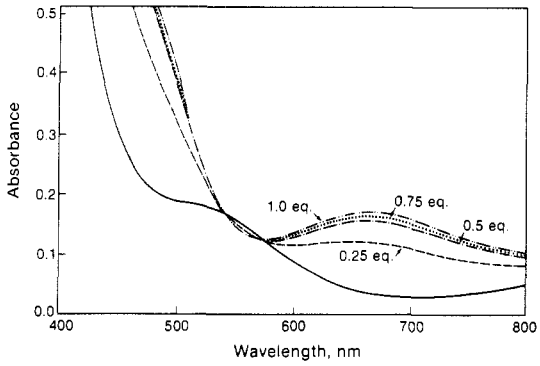

Figure 5. Spectrophotometric titration of 1 mM $Mn^{III}(PA)_2(acac)$ with *N*-Oct-disalH_2 in MeCN.

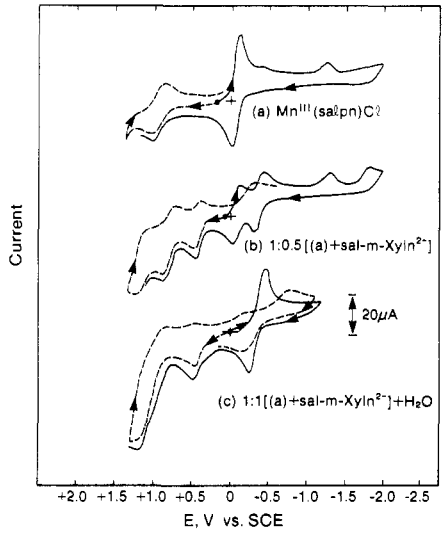

Figure 6. Electrochemical titration of 2 mM Mn^{III}(salpn)Cl with sal-*m*-$Xyln^{2-}$ in MeCN (0.1 M TEAP) at a glassy-carbon electrode.

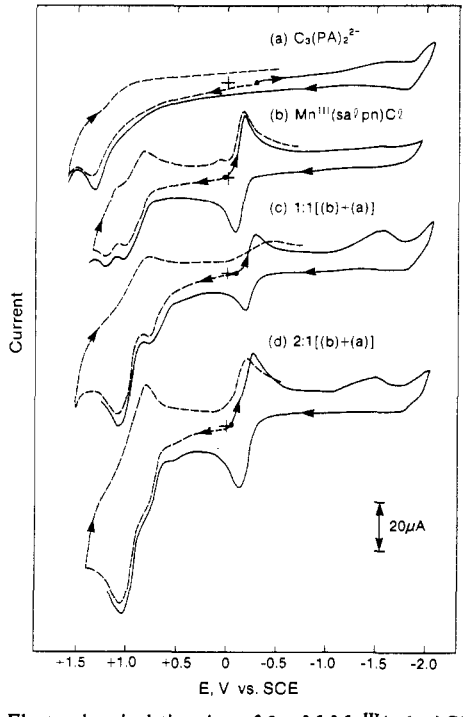

Figure 7. Electrochemical titration of 2 mM Mn^{III}(salpn)Cl with $C_3(PA)_2^{2-}$ in MeCN (0.1 M TEAP) at a glassy-carbon electrode.

Reaction of Mn^{III}(salpn)Cl with $[Me_4N]_2$[sal-*m*-Xyln] and $[Me_4N]_2[C_3(PA)_2]$. The Mn^{III}(salpn)Cl complex has a reversible reduction at −0.06 V vs SCE and a reversible oxidation at +0.97 V (Figure 6). Addition of 0.5 equiv of sal-*m*-$Xyln^{2-}$ [generated in situ by the addition of $(Me_4N)OH$ to sal-*m*-$XylnH_2$] per Mn^{III}(salpn)Cl yields a product with two reversible oxidations at +0.45 and +0.85 V vs SCE and two reversible reductions at +0.08 and −0.40 V vs SCE (Figure 6). Addition of a small amount of water to this solution causes the oxidation waves to become irreversible; the reverse scan yields a broad reduction peak at −0.74 V vs SCE [the peak current is decreased when argon is bubbled through the solution (Figure 6)].

Figure 7 illustrates that a carboxylate group of $[Me_4N]_2[C_3(PA)_2]$ is oxidized at +1.26 V vs SCE. The cyclic voltammogram of Mn^{III}(salpn)Cl is shown in Figure 7b. Addition of 1 equiv of Mn^{III}(salpn)Cl (curve b) to a solution of $[Me_4N]_2[C_3(PA)_2]$ yields a product with a reversible reduction at +0.18 V vs SCE, a reversible oxidation at +0.85 V, and an irreversible oxidation at +1.05 V (curve c). The heights for each of these peaks increases upon addition of more (Mn^{III}salpn)Cl up to maximum of 2 Mn/$[C_3(PA)_2]^{2-}$ (curve d). The 1:1 combination of $(Me_4N)PA$ and Mn^{III}(salpn)Cl yields a product solution that has the same electrochemical response as that of Figure 7d.

Reaction of $[(\mu\text{-}O)_2(Mn^{III/IV}(bpy)_2)_2]^{3+}$ with $(Me_4N)PA$. Addition of two picolinate (PA^-) ions to a solution of $[(\mu\text{-}O)_2$-

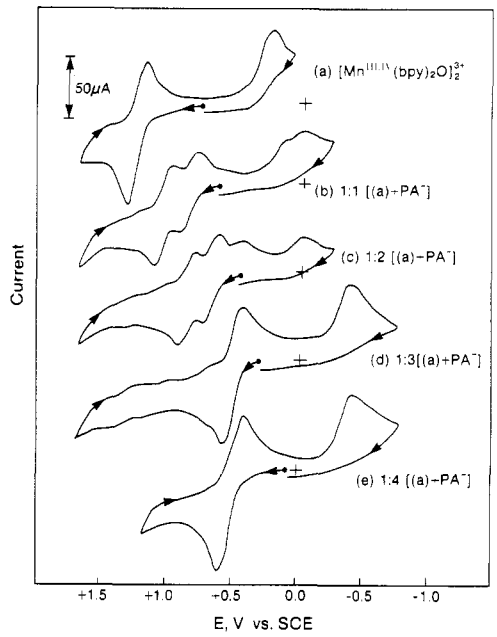

Figure 8. Electrochemical titration of 5 mM $[Mn^{III/IV}(bpy)_2O]_2^{3+}$ with PA^- in MeCN (0.1 M TEAP) at a glassy-carbon electrode.

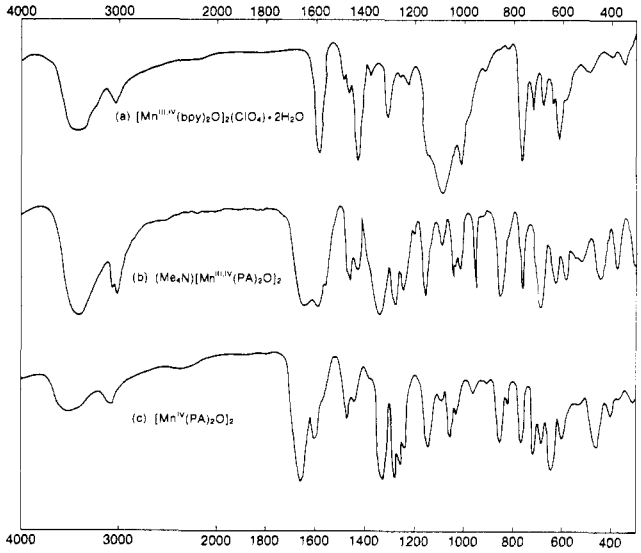

Figure 9. Infrared spectra: (a) $[Mn^{III/IV}(bpy)_2O]_2(ClO_4)_3$; (b) $(Me_4N)[Mn^{III/IV}(PA)_2O]_2$; (c) $[Mn^{IV}(PA)_2O]_2$.

Table I. Electrochemical and Spectroscopic Data for Mono- and Binuclear Manganese(III) Complexes in Anhydrous Acetonitrile (0.1 M Tetraethylammonium Perchlorate)[a]

A. $[Mn^{III}(PA)_2(acac)]$ Adducts

complex[b]	$E_{1/2}$, V vs NHE: $Mn^{II}(L_1^-)(L_2^{\bullet})/Mn^{II}(L_1^-)(L_2^-)$ ($Mn^{III/II}$)	$E_{1/2}$, V vs NHE: $Mn^{II}(L_1^-)(L_2^{\bullet})/Mn^{II}(L_1^{\bullet})(L_2^{\bullet})$ ($Mn^{III/IV}$)	λ_{max}, nm (ϵ, M^{-1} cm^{-1})[c]
1. Mononuclear			
$Mn^{II}(PA^-)_2(acac^{\bullet})$ $[Mn^{III}(PA)_2(acac)]$	+0.41	+1.45	520 (190)
$Mn^{II}(PA^-)(salen^{\bullet-})$ $[Mn^{III}(PA)(salen)]$	+0.08	+0.96 (+1.37)[d]	580 (220)
$Mn^{II}(PA^-)(salpn^{\bullet-})$ $[Mn^{III}(PA)(salpn)]$	+0.02	+0.97 (+1.34)[d]	576 (414)
2. Binuclear			
$[Mn^{II}(PA^-)_2]_2$(*N*-Oct-disal$^{\bullet}$) $\{[Mn^{III}(PA)_2]_2$(*N*-Oct-disal)$\}$	+0.24 (−0.04)[e]	+1.29 (1.64)[d]	664 (180)
$\{[(Mn^{II}(PA^-)_2]_2$($^{\bullet}$sal-*m*-Xyln$^{\bullet}$) $\{[Mn^{III}(PA)_2]_2$(sal-*m*-xyln)$\}$	+0.24 (−0.04)[e]	+1.35 (+1.70)[d]	605 (130)
$[(Mn^{II}(PA^-)_2]_2$($^{\bullet}$salhn$^{\bullet}$) $\{[Mn^{III}(PA)_2]_2$(salhn)$\}$	+0.26 (−0.04)[e]	+1.31 (+1.71)[d]	650 (130)
$[(Mn^{II}(PA^-)_2]_2$($^{\bullet}$disal$^{\bullet}$) $\{[(Mn^{III}(PA)_2]_2$(disal)$\}$	+0.44 (+0.16)[e]	+1.49[d]	515 (280)

B. Mn^{III}(salpn)(Cl) Adducts

complex[a]	$E_{1/2}$, V vs NHE: $Mn^{II}(L_1^-)(L_2^{\bullet})/Mn^{II}(L_1^-)(L_2^-)$ ($Mn^{III/II}$)	$E_{1/2}$, V vs NHE: $Mn^{II}(L_1^-)(L_2^{\bullet})/Mn^{II}(L_1^{\bullet})(L_2^{\bullet})$ ($Mn^{III/IV}$)	λ_{max}, nm (ϵ, M^{-1} cm^{-1})[c]
1. Mononuclear			
$Mn^{II}(salpn^{\bullet-})(Cl^-)$ $[Mn^{III}(salpn)(Cl)]$	+0.18 (+0.13)[f]	+1.21 (+1.17)[f]	635 (275)
$Mn^{II}(salpn^{\bullet-})(PA^-)$ $[Mn^{III}(salpn)(PA)]$	+0.03	+0.99, +1.29[d]	576 (400)
2. Binuclear			
$[Mn^{II}(salpn^{\bullet-})]_2$(sal-*m*-$Xyln^{2-}$) $\{[Mn^{III}(salpn)]_2$(sal-*m*-Xyln)$\}$	+0.16, −0.16	+0.69, +1.09	600 (sh)
$[(Mn^{II}(salpn^{\bullet-})]_2[C_3(PA^-)_2]$ $\{[Mn^{III}(salpn)]_2[C_3(PA)_2]\}$	+0.06[f]	+1.09,[f] +1.29[d,f]	560 (424)

C. (μ-O)$_2$-Bridged Complexes (Binuclear)

complex[b]	$E_{1/2}$, V vs NHE: $[Mn^{II}_2(\mu\text{-}O)(\mu\text{-}O^{\bullet-})]/[Mn^{II}_2(\mu\text{-}O^{\bullet-})_2]$ ($Mn^{IV/III}/Mn^{III/III}$)	$E_{1/2}$, V vs NHE: $[Mn^{II}_2(\mu\text{-}O)(\mu\text{-}O^{\bullet-})]/[Mn^{II}_2(\mu\text{-}O)_2]$ ($Mn^{IV/III}/Mn^{IV/IV}$)	λ_{max}, nm (ϵ, M^{-1} cm^{-1})
$\{(\mu\text{-}O)(\mu\text{-}O^{\bullet-})[Mn^{II}(bpy)_2]_2\}^{3+}$ $\{(\mu\text{-}O)_2[Mn^{III/IV}(bpy)_2]_2\}^{3+}$	+0.59[e]	+1.57	684 (593)
$\{(\mu\text{-}O)(\mu\text{-}O^{\bullet-})[Mn^{II}(PA^-)(bpy)]_2\}^{+}$ $\{(\mu\text{-}O)_2[Mn^{III/IV}(PA)(bpy)]_2\}^{+}$	+0.24[e]	+0.84, +1.04	
$\{(\mu\text{-}O)(\mu\text{-}O^{\bullet-})[Mn^{II}(PA^-)_2]_2\}^{-}$ $\{(\mu\text{-}O)_2[Mn^{III/IV}(PA)_2]_2\}^{-}$	−0.18[e]	+0.77	530 (35) 630 (sh)

[a] The redox couples represent formulations for ligand-centered redox products and denote charge distribution on both metal and ligand(s). The more traditional metal-centered electron-transfer formulation is shown below in parentheses. [b] PA, picolinate; acac, acetylacetonate; bpy, 2,2′-bipyridyl. [c] Molar absorptivity per Mn. [d] Irreversible voltammogram, E_{pa} (scan rate 0.1 V s^{-1}). [e] Irreversible voltammogram, E_{pc} (scan rate 0.1 V s^{-1}). [f] DMF solvent.

$[Mn^{III/IV}(bpy)_2)_2]^{3+}$ yields a complex with an irreversible reduction 0.0 V vs SCE and two reversible oxidations at +0.6 and +0.8 V (Figure 8). Addition of two more PA^- ions yields a second complex that has an irreversible reduction at −0.42 V vs SCE and a reversible oxidation at +0.53 V. The electrochemistry and UV/visible spectrum of this solution are the same as those for a solution prepared from the isolated $(Me_4N)\{(\mu\text{-}O)_2[Mn^{IV/III}(PA)_2]_2\}$ complex. Infrared spectra of the isolated 4:1 adduct confirms the incorporation of PA^- and the preservation of the bis(μ-oxo) bridge (Figure 9).

Discussion and Conclusions

The results of Figures 2 and 3 and Table I indicate that salenH_2 and salpnH_2, form 1:1 mononuclear adducts with $[Mn^{III}(PA)_2(acac)]$ via ligand displacement of $acac^-$ and PA^- (for example, see eq 1). In contrast, binuclear products result when the ligand has steric constraints to tetradentate bonding to a single metal center. Thus, *N*-Oct-disalH_2, sal-*m*-XylnH_2, disalH_2, and salhnH_2 each combine with two $Mn^{III}(PA)_2(acac)$ complexes via displacement of $acac^-$ to form discrete, bridged binuclear compounds (Figures 4 and 5 and Table I; for example, see eq 2). The

$$[Mn^{III}(PA)_2(acac)] + \text{salpn}H_2 + 2OH^- \rightarrow Mn^{III}(\text{salpn})(PA) + acac^- + PA^- + H_2O \quad (1)$$

$$2[Mn^{III}(PA)_2(acac)] + N\text{-Oct-disal}H_2 \rightarrow [Mn^{III}(PA)_2]_2(N\text{-Oct-disal}) + 2acacH \quad (2)$$

combinations of two mononuclear Mn^{III}(salpn)Cl complexes with sal-*m*-$Xyln^{2-}$ and with $C_3(PA)_2^{2-}$ (Figure 2) yield the corresponding bridged, binuclear complexes (eq 3 and 4).

$$2Mn^{III}(\text{salpn})Cl + \text{sal-}m\text{-}Xyln^{2-} \rightarrow [Mn^{III}(\text{salpn})]_2(\text{sal-}m\text{-Xyln}) + 2Cl^- \quad (3)$$

$$2Mn^{III}(\text{salpn})Cl + C_3(PA)_2^{2-} \rightarrow [Mn^{III}(\text{salpn})]_2(C_3(PA)_2) + 2Cl^- \quad (4)$$

The third class of binuclear manganese complexes results from substitution of the bpy groups in $[(\mu\text{-}O)_2(Mn^{III/IV}(bpy)_2)_2]^{3+}$ by the picolinate anion (PA^-) (eq 5 and 6).

$$\{(\mu\text{-O})_2[Mn^{III/IV}(bpy)_2]_2\}^{3+} + 2PA^- \rightarrow \{(\mu\text{-O})_2[Mn^{III/IV}(bpy)(PA)]_2\}^{+} + 2bpy \quad (5)$$

1

$$\{(\mu\text{-O})_2[Mn^{III/IV}(bpy)_2]_2\}^{3+} + 4PA^- \rightarrow \{(\mu\text{-O})_2[Mn^{III/IV}(PA)_2]_2\}^{-} + 4bpy \quad (6)$$

2

The infrared spectrum of **2** (Figure 9) has bands that are characteristic of PA^- at 1650, 1345, 850, and 690 cm^{-1} as well bands at 645 cm^{-1} due to the bis(μ-oxo) linkage and at 3000 cm^{-1} due to the tetramethylammonium ion. The infrared spectrum of $[Mn^{IV}(PA)_2O]_2$ also has similar features (Figure 9).

Redox Thermodynamics for Mononuclear and Binuclear Manganese Complexes. The mononuclear complexes of Table I are neutral and each exhibit a reversible reduction (from +0.41 V vs NHE for $[Mn^{III}(PA)_2(acac)$ to +0.02 V for $Mn^{III}(PA)(salpn)$. The mononuclear tris(picolinato) complex $[Mn^{III}(PA)_3]$ exhibits a reversible reduction at +0.62 V vs NHE. A parallel study[29] has demonstrated that the redox chemistry for a number of manganese(II) complexes (including $[Mn^{II}(PA)_3]^-$ and $[Mn^{II}(PA)_2(acac)]^-$ is ligand-centered and the potentials are determined by the redox chemistry of the ligand and the electrostatic charge of the complex. The net transformation is the conversion of a ligand donor bond (L^-) to the ligand radical ($L^\bullet$), which pairs with an unpaired metal d electron to form a covalent bond. Thus, free PA^- is oxidized to $PA^\bullet$ at +1.65 V vs NHE whereas $Mn^{II}(PA)_3^-$ is oxidized to $[Mn^{II}(PA^-)_2(PA^\bullet) \equiv Mn^{III}(PA^-)_3]$ at +0.62 V vs NHE.[8] The shift in potential of −1.03 V is a measure of the covalent bond energy (1.03 × 23.1 = 23.8 kcal) for the d–p bond that results from the two unpaired electrons.

Hence, in the case of the complexes of Table I, a more realistic formulation would have the manganese in the Mn(II) oxidation state with the most easily oxidized ligand bound as a ligand radical. The formation reactions that are written as anionic ligand substitutions, (e.g., eq 1 and 2, actually involve oxidation of the Schiff-base ligand by the acetylacetoxyl radical of $[Mn^{II}(PA)_2(acac^\bullet)]$ (a redox process as opposed to a simple substitution). The resulting ligand-centered redox formulations are given in Table I and provide a rationale for the two one-electron reductions of the binuclear complexes in Table I. Each is due to the addition of an electron to the two bridging ligand–radical (covalent p–d bond) centers. In the case of the $[L_2Mn^{II}](\mu\text{-}O^{\bullet-})_2$ complexes, the most easily oxidized ligands are the bridging (μ-$O^{\bullet-}$) groups.

With these oxidized-ligand formulations for the complexes of Table I, the reversible oxidation couples (indicated as Mn^{III}/Mn^{IV}) actually represent additional oxidation of bound ligands. Thus, for $[Mn^{II}(PA^-)_2(^\bullet acac)]$, the reversible oxidation at +1.45 V vs NHE yields an oxidized picolinate ($PA^- \rightarrow PA^\bullet$) covalently bound to an unpaired manganese(II) d electron, $[Mn^{II}(PA^-)(^\bullet PA)(acac^\bullet)]^+$. Similarly, for $[Mn^{II}PA^-)_2(PA^\bullet)]$ the reversible oxidation at +1.61 V vs NHE[8] (to give $[Mn^{II}(PA^-)(PA^\bullet)_2]^+$) reflects the fact that PA^- is more difficult to oxidize and that the Mn(d)–L(p) bond energies are about the same for $PA^\bullet$ and $acac^\bullet$.

The binuclear complexes of Table I now are formulated with both donor centers of the bridging Schiff base oxidized to neutral radicals (e.g., $\{[Mn^{II}PA^-)_2]_2(^\bullet N\text{-Oct-disal}^\bullet)\}$. Hence, the positive oxidation potentials are due to the removal of an electron from a coordinated picolinate ion, which forms a covalent bond with another manganese(II) unpaired d electron.

The new formulation for the $[(Mn^{II}salpn^{\bullet-})_2(sal\text{-}m\text{-}Xyln^{2-})]$ means that the double oxidation peaks are due to the sequential conversion of the bridging ligand $[(sal\text{-}m\text{-}Xyln)^{2-}]$ to $(sal\text{-}m\text{-}Xyln^\bullet)^-$ and finally to $(^\bullet sal\text{-}m\text{-}Xyln^\bullet)$ (Table I). With the redox-inert $[C_3(PA)_2]^{2-}$ bridging ligand, the two one-electron-oxidation peaks for $[Mn^{II}(salpn^{\bullet-})]_2[C_3(PA^-)_2]$ are due to the respective conversion of the two $Mn^{II}(salpn^{\bullet-})$ moieties to $Mn^{II}(^\bullet salpn^\bullet)$ centers.

For the bis(μ-oxo)-bridged systems of Table IC, the oxidation peak is due to the conversion of the bridging ($O^{\bullet-}$) groups to ($^\bullet O^\bullet$); the shift in potential from +1.57 V vs NHE for L = bpy to +0.77 V for L = PA^- reflects the change in net charge for the complex from +3 to −1. [^-OH is oxidized at +0.6 V vs NHE when bound to Mn(II) in the $Mn(Ph_3PO)_4(^-OH)_3^-$ complex].[30]

Relation to the H_2O Oxidation Center of PSII. To oxidize H_2O to O_2 at pH 7 in a biomembrane requires a minimum oxidation potential of ~0.6 V vs NHE and needs to be accomplished via a concerted 2-, 3-, or 4e process. Thus, a binuclear manganese complex is believed to be a minimal requirement. Of the systems characterized in Table I, the $[Mn^{II}(salpn^{\bullet-})]_2(sal\text{-}m\text{-}Xyln^{2-})$ complex has the most reversible redox chemistry (Figure 6b) with two one-electron reductions (+0.16 and −0.16 V vs NHE) and two one-electron oxidations (+0.69 and +1.09 V vs NHE). The latter represent the sequential oxidation of the bridging Schiff-base ligand to ($^\bullet sal\text{-}m\text{-}Xyln^\bullet$) and give an oxidized complex with a sufficiently positive potential to oxidize water at neutral pH (pH 9 for a PA^-/PAH buffer in MeCN).[31] The addition of water to the complex solution causes the oxidation peaks to become irreversible, and the reverse scan indicates the complex has been reduced via the oxidation of H_2O to give O_2 (reduction peak at −0.6 V vs NHE that is removed by an argon purge of the solution). A possible redox process involves the concerted conversion of water to oxygen by the fully oxidized complex (eq 7), where the

$$\{[Mn^{II}(salpn^{\bullet-})]_2(^\bullet sal\text{-}m\text{-}Xyln^\bullet)\}^{2+} + 2H_2O + 4PA^- \rightarrow \{[Mn^{II}(salpn^{2-})]_2(sal\text{-}m\text{-}Xyln^{2-})\}^{2-} + O_2 + 4PAH \quad (7)$$

($-4e^-$ / $+4e^-$)

PA^-/PAH system models the effective buffering capacity of the thylakoid matrix.

An alternative model for the H_2O-oxidizing cofactor of PSII consists of two two-manganese groups; one a 4e charge accumulation center and the other a template to hold two water molecules such that O–O bond formation is facilitated upon oxidation via the manganese center. A similar process may also pertain in the reaction of MnO_4^- with MnO_2.

$$2MnO_4^- + 5MnO_2 + 16H^+ \rightarrow 7Mn^{II} + 8H_2O + 5O_2 \quad (8)$$

Thus, in terms of redox thermodynamics, the oxidized binuclear complex $[Mn^{II}(salpn^{\bullet-})]_2(^\bullet sal\text{-}m\text{-}Xyln^\bullet)^{2+}$ represents a unique four-electron charge accumulation system. The other binuclear systems of Table I, when fully oxidized, act as two-electron oxidants $[(\mu\text{-O})_2(Mn^{II}L_2)_2]$ and as four-electron oxidants $([Mn^{II}(^\bullet salpn^\bullet)]_2[C_3(PA)_2^{2-}]^{2+}$ and $[Mn^{II}(PA^\bullet)(PA^-)]_2(^\bullet sal\text{-}m\text{-}Xyln^\bullet)^{2+})$. However, the potential for full oxidation of the latter system is well beyond the limits of the potential generated by the primary photoact in PSII.[32] The $[Mn^{II}(salpn^{\bullet-})]_2[C_3(PA)_2^{2-}]$ complex appears to be a promising model for 4e charge accumulation. Further studies are in progress with it and the $[Mn^{II}(salpn^{\bullet-})]_2(sal\text{-}m\text{-}Xyln^{2-})$ complex as oxidants of manganese complexes with coordinated water molecules, e.g., $[Mn^{II}(PA)_2(OH_2)_2]$.

Acknowledgment. This work was supported by the National Institutes of Health under Grant No. GM-36289 and the National Science Foundation under Grant No. CHE-8516247.

Registry No. $[C_3(pyO)_2]$, 34049-15-5; $[C_3(pyCN)_2]$, 112988-01-9; $[C_3(PAH)_2]$, 112988-02-0; $[Mn^{III}(salpn)(Cl)]$, 99568-94-2; $[Mn^{II}(salpn)Cl]^-$, 112988-27-9; $[Mn^{IV}(salpn)Cl]^+$, 112988-28-0; $(Me_4N)\{(\mu\text{-O})_2[Mn^{III/IV}(PA)_2]_2\}$, 112988-04-2; $\{(\mu\text{-O})_2[Mn^{IV}(PA)_2]_2\}$, 112988-05-3; $\{(\mu\text{-O})_2[Mn^{III}(PA)_2]_2\}^{2-}$, 112988-33-7; $\{(\mu\text{-O})_2[Mn^{III/IV}(bpy)_2]_2\}(ClO_4)_3$, 49729-96-6; $\{(\mu\text{-O})_2[Mn^{III}(bpy)_2]_2\}^{2+}$, 62365-00-8; $\{(\mu\text{-O})_2[Mn^{IV}(bpy)_2]_2\}^{4+}$, 62364-98-1; $(\mu\text{-O})_2[Mn^{IV}(phen)_2]_2(ClO_4)_4$, 62412-52-6; $[Mn^{III}(PA)_2(acac)]$, 79257-38-8; $[Mn^{II}(PA)_2(acac)]^-$, 112988-15-5; $[Mn^{IV}(PA)_2(acac)]^+$, 112988-16-6; $[Mn^{III}(PA)(salen)]$, 112988-06-4; $[Mn^{II}(PA)(salen)]^-$, 113008-21-2; $[Mn^{IV}(PA)(salen)]^+$, 112988-17-7; $[Mn^{III}(PA)(salpn)]$, 112988-07-5; $[Mn^{II}(PA)(salpn)]^-$, 112988-18-8; $[Mn^{IV}(PA)(salpn)]^+$, 112988-19-9; $\{[Mn^{III}(PA)_2]_2(N\text{-Oct-disal})\}$,

(29) Richert, S.; Tsang, P. K. S.; Sawyer, D. T. *Inorg. Chem.*, in press.

(30) Tsang, P. K. S.; Cofré, P.; Sawyer, D. T. *Inorg. Chem.* **1987**, *26*, 3604.

(31) Cofré, P.; Sawyer, D. T. *Anal. Chem.* **1986**, *58*, 1057.

(32) Knox, R. S. *Primary Processes of Photosynthesis*; Elsevier: Amsterdam, 1977; p 56.

112988-08-6; $\{[Mn^{II}(PA)_2]_2(N\text{-Oct-disal})\}^{2-}$, 112988-20-2; $\{[Mn^{IV}(PA)_2]_2(N\text{-Oct-disal})\}^{2+}$, 112988-21-3; $\{[Mn^{III}(PA)_2]_2(sal\text{-}m\text{-Xyln})\}$, 112988-09-7; $\{[Mn^{II}(PA)_2]_2(sal\text{-}m\text{-Xyln})\}^{2-}$, 113008-22-3; $\{[Mn^{IV}(PA)_2]_2(sal\text{-}m\text{-Xyln})\}^{2+}$, 112988-22-4; $\{[Mn^{III}(PA)_2]_2(salhn)\}$, 112988-10-0; $\{[Mn^{II}(PA)_2]_2(salhn)\}^{2-}$, 112988-23-5; $\{[Mn^{IV}(PA)_2]_2(salhn)\}^{2+}$, 112988-24-6; $\{[Mn^{III}(PA)_2]_2(disal)\}$, 112988-11-1; $\{[Mn^{II}(PA)_2]_2(disal)\}^{2-}$, 112988-25-7; $\{[Mn^{IV}(PA)_2]_2(disal)\}^{2+}$, 112988-26-8; $\{[Mn^{III}(salpn)]_2(sal\text{-}m\text{-Xyln})\}$, 112988-12-2; $\{[Mn^{II}(salpn)]_2(sal\text{-}m\text{-Xyln})\}^{2-}$, 113008-23-4; $\{[Mn^{IV}(salpn)]_2(sal\text{-}m\text{-Xyln})\}^{2+}$, 112988-29-1; $\{[Mn^{III}(salpn)]_2[C_3(PA)_2]\}$, 112988-13-3; $\{[Mn^{II}(salpn)]_2[C_3(PA)_2]\}^{2-}$, 112988-30-4; $\{[Mn^{IV}(salpn)]_2[C_3(PA)_2]\}^{2+}$, 113008-24-5; $\{(\mu\text{-}O)_2[Mn^{III/IV}(PA)(bpy)]_2\}^{+}$, 112988-14-4; $\{(\mu\text{-}O)_2[Mn^{III}(PA)(bpy)]_2\}$, 112988-31-5; $\{(\mu\text{-}O)_2[Mn^{IV}(PA)(bpy)]_2\}^{2+}$, 112988-32-6; H_2O, 7732-18-5; O_2, 7782-44-7; 4,4′-trimethylenebis(pyridine), 17252-51-6.

Contribution from the Department of Inorganic Chemistry, Indian Association for the Cultivation of Science, Calcutta 700032, India

Aromatic Hydroxylation via Cyclometalation. Metaloxylation of Palladated 2-(Alkylsulfinyl)azobenzenes

Chittaranjan Sinha, Debkumar Bandyopadhyay, and Animesh Chakravorty*

Received June 15, 1987

Several azo sulfoxide ligands belonging to the class 2-(sulfinyl)azobenzenes (**3**) have been synthesized: $C_6H_4(R')—N{=}N—C_6H_4X$ (R′ = H, 4′-Me, 5′-Me; X = 2-S(O)R, R = Me, CH_2Ph). These react with Na_2PdCl_4 in ethanol, affording brown-red cyclopalladated species having the coordination sphere Pd(C,N,S)Cl (**4**). The mode of ligand binding is established with the help of high-resolution ^1H NMR and IR data. In chloroform solution **4** reacts with *m*-chloroperbenzoic acid (mCPBA), resulting in high-yield regiospecific oxidation (metaloxylation) of the C–Pd moiety into C–O–Pd. The resulting pink-violet Pd(O,N,S)Cl complexes (**5**) have been characterized spectroscopically and in one case by independent synthesis via a nonoxidative route. From **5** the free hydroxyazo ligand (**6**) can be liberated via reductive (hydrazine) elimination of the metal. The metalation–metaloxylation–demetalation sequence thus affords a high-yield route for regiospecific aromatic hydroxylation of the azobenzenes under consideration. The kinetics of the metaloxylation reaction has been examined in two cases. The rate law is $d[5]/dt = k[4]\cdot[mCPBA]$. The enthalpy of activation is small (~9 kcal). The large negative entropy of activation (~−30 eu) suggests an associative mechanism. It is proposed that in the transition state mCPBA binds to the metal center via peroxy oxygen followed by heterolytic cleavage of the O–O bond and oxygen insertion into the Pd–C bond.

Introduction

A major goal of current chemical research is to achieve metal-catalyzed activation of the C–H bond. So activated, the bond is a potent site for chemoselective transformations that are otherwise difficult or impossible to achieve. Hydroxylation of the aromatic ring (eq 1)is an example per se. Metal ion mediation

$$Ar–H \rightarrow Ar–OH \qquad (1)$$

of one form or another is frequently obligatory for this reaction to occur either in vivo or in vitro.[1-9] This work concerns the metal-promoted aromatic hydroxylation route stated in eq 2. In

$$Ar–H \xrightarrow{i} Ar–M \xrightarrow{ii} ArOM \xrightarrow{iii} ArOH \qquad (2)$$

step i arene C–H activation[10] affords Ar–M into which oxygen is inserted in step ii. Subsequent demetalation (step iii) affords the net reaction of eq 1. Very little is however known about oxygen insertion into the Ar–M bond, step ii.[3,11-13] This has seriously limited practical application of eq 2 for achieving aromatic hydroxylation.

Recently we have initiated a program for defining the scope and nature of the reaction Ar–M → Ar–OM, which has been called aromatic metaloxylation. Certain cyclopalladated azobenzenes were shown to undergo facile metaloxylation by *m*-chloroperbenzoic acid (mCPBA). In the particular case of azobenzene thioether complexes having coordination sphere **1**, the

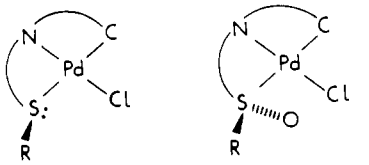

1 **2**

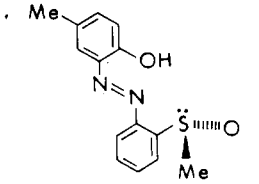

6

Pd–C bond was selectively oxygenated but the sulfur center remained unreactive and sulfoxide formation did not occur.[3]

Herein we describe the successful synthesis of metalated azo sulfoxide species of coordination type **2** by metalation of preformed ligands. The major point of interest is that both in terms of high yields and mechanistic simplicity **2** represents a model substrate

(1) Hamilton, G. A. *Molecular Mechanisms of Oxygen Activation*; Hayaishi, O., Ed.; Academic: New York, 1974; p 405.
(2) Sheldon, R. A.; Kochi, J. K. *Metal-Catalyzed Oxidation of Organic Compounds*; Academic: New York, 1981; p 236.
(3) Mahapatra, A. K.; Bandyopadhyay, D.; Bandyopadhyay, P.; Chakravorty, A. *Inorg. Chem.* **1986**, *25*, 2214–2221 and references therein.
(4) Kazandjian, R. Z.; Klibanov, A. M. *J. Am. Chem. Soc.* **1985**, *107*, 5448–5450.
(5) Wilcox, D. E.; Porras, A. G.; Hwang, Y. T.; Lerch, K.; Winkler, M. E.; Solomon, E. I. *J. Am. Chem. Soc.* **1985**, *107*, 4015–4027.
(6) Korzekwa, K.; Trager, W.; Gouterman, M.; Spangler, D.; Loew, G. H. *J. Am. Chem. Soc.* **1985**, *107*, 4273–4279.
(7) Mimoun, H.; Saussine, L.; Daire, E.; Postel, M.; Fischer, J.; Weiss, R. *J. Am. Chem. Soc.* **1983**, *105*, 3101–3110.
(8) Srivatsa, G. S.; Sawyer, D. T. *Inorg. Chem.* **1985**, *24*, 1732–1734.
(9) Kunai, A.; Hata, S.; Ito, S.; Sasaki, K. *J. Am. Chem. Soc.* **1986**, *108*, 6012–6016.
(10) Cope, A. C.; Siekman, R. W. *J. Am. Chem. Soc.* **1965**, *87*, 3272–3273. Bruce, M. I. *Angew. Chem., Int. Ed. Engl.* **1977**, *16*, 73–86. Parshall, G. W. *Acc. Chem. Res.* **1970**, *3*, 139–141. Parshall, G. W. *Acc. Chem. Res.* **1975**, *8*, 113–117. Jones, W. D.; Feher, F. J. *J. Am. Chem. Soc.* **1985**, *107*, 620–631. Omae, I. *Chem. Rev.* **1979**, *79*, 287–321. Omae, I. *Organometallic Intramolecular Coordination Compounds*; Elsevier: New York, 1986. Cooper, N. J.; Green, M. L. H.; Mehtab, R. *J. Chem. Soc., Dalton Trans.* **1979**, 1557–1562. Berry, M.; Elmitt, K.; Green, M. L. H. *Ibid.* **1979**, 1950–1958. Werner, R.; Werner, H. *Angew. Chem., Int. Ed. Engl.* **1981**, *20*, 793–794.
(11) Ryabov, A. D. *Synthesis* **1985**, 233–252.
(12) Mahapatra, A. K.; Bandyopadhyay, D.; Bandyopadhyay, P.; Chakravorty, A. *J. Chem. Soc., Chem. Commun.* **1984**, 999–1000.
(13) Grigor, B. A.; Neilson, A. *J. Organomet. Chem.* **1977**, *129*, C17–C19.

0020-1669/88/1327-1173$01.50/0